# Air pocket removal from downward sloping pipes

I.W.M.(Ivo) Pothof (IAHR member)[1,2], F.H.L.R. (Francois) Clemens[2]

[1]Deltares, Netherlands, ivo.pothof@deltares.nl
[2]Delft University of Technology, Netherlands, F.H.L.R.Clemens@TUDelft.nl

## ABSTRACT

Air-water flow is an undesired condition in water pipelines and hydropower tunnels. Water pipelines and wastewater pressure mains in particular are subject to air pocket accumulation in downward sloping reaches, such as inverted siphons or terrain slopes. Air pockets cause energy losses and an associated capacity reduction. Despite its practical relevance, many phenomena associated with air-water flow in downward sloping pipe reaches are still poorly understood. Deltares and Delft University of Technology have investigated the co-current flow of air and water in twelve different large-scale facilities. Pothof and Clemens have recently developed a numerical model for the total air discharge by flowing water in downward sloping pipes. The model has been validated against the experimental data on co-current air-water flow and available literature. This paper presents new experimental data on the breakdown and removal of large air pockets. The experimental results are compared with the numerical model. The observed disagreement is analysed and discussed. The main conclusion is that the numerical model predicts the air pocket breakdown rate with reasonable accuracy.

## KEYWORDS

air discharge, air pockets, downward pipe angle, pipe flow, two-phase flow, wastewater.

## 1 INTRODUCTION

### 1.1 Background

Air-water flow is an undesired condition in many systems for the transportation of water or wastewater. Air in storm water tunnels may get trapped and negatively affect the system (Vasconcelos and Wright 2009). Air pockets in hydropower tunnels or sewers may cause blow-back events and inadmissible pressure spikes (Capart et al. 1997). Water pipes and wastewater pressure mains in particular are subject to air pocket formation in downward-sloping reaches, such as inverted siphons or terrain slopes. Air pocket accumulation causes energy losses and an associated capacity reduction (Lubbers 2007). The extra head loss due to the air pocket presence is roughly equal to the vertical distance between the pocket nose and tail (Lubbers and Clemens 2007). Air pockets in pressurised wastewater mains often are not expelled via air valves, because:

- Hazardous gases may be released;
- Air valves do often not cope with the composition of wastewater (floating debris in particular) and remain closed or, even worse, remain open after the air has been expelled;
- Pressure may be sub-atmospheric at the intended air valve location, and
- Preferred air valve location is on private property or on an inaccessible location for maintenance.

Therefore, air must be transported by the flowing water in many pressurised wastewater mains.

The recent research efforts on air accumulation in storm water tunnels (Vasconcelos and Wright 2009) or in hydropower tunnels (Wickenhäuser and Kriewitz 2009) confirm the existing knowledge gap on the motion of elongated air pockets in downward sloping pipes. Whereas in horizontal and in upwardly inclined pipes all entrained air is transported with the water flow, the air in downward sloping pipes can move in both directions. Knowledge on air pocket motion in downward sloping pipes is essential for the proper venting of pressurized pipes and for the prevention of severe blow-back events in stormwater tunnels or hydropower stations.

### 1.2 Literature overview

The transport of air through downward sloping pipes has been investigated by a number of researchers (Escarameia 2007, Gandenberger 1957, Kalinske and Bliss 1943, Kent 1952). These researchers focused on the air entrainment in a hydraulic jump at the end of a gas accumulation, which is the dominant transport mechanism in the blow-back flow regime. Unfortunately, the investigators neglected the importance of the gas pocket length in relation to the slope length in order to predict the net air discharge at the bottom of the downward sloping section.

Zukoski (1966) has investigated the influence of the viscosity and surface tension on bubble rise velocities. The rise velocity of elongated bubbles in a stagnant liquid, known as the drift velocity, is closely related to water velocity required to start moving an air pocket in downward direction; the latter is known as the clearing velocity. Bendiksen (1984) has experimentally shown in small diameter pipes ($D$ = 0.0242 m) that the drift velocity $v_d$ and clearing velocity $v_c$ are nearly identical in pipes with an inclination up to 30°.

$$0.98 v_c = v_d \tag{1}$$

The water flow number $\mathsf{F}_w$ is defined as

$$\mathsf{F}_w = \frac{v_{sw}}{\sqrt{gD}} \tag{2}$$

where $v_{sw}$ is the superficial water velocity (i.e. $v_{sw} = Q_w / (0.25\ \pi D^2)$) and $D$ is the pipe diameter. The air flow number $\mathsf{F}_g$ is non-dimensionalised analogously. The clearing flow number $\mathsf{F}_c$ is the non-dimensional clearing velocity.

The clearing velocity becomes independent of the pipe diameter if $D$ > 0.19 m at which the clearing flow number is $\mathsf{F}_c$ = 0.9 (Pothof and Clemens 2010). The flow number (or pipe Froude number) $\mathsf{F}_w$ is the dominant dimensionless number, because the Reynolds influence on the drift velocity is limited to pipes with D < 0.004 m for air-water flows (Zukoski 1966). Scale effects due to surface tension were only investigated by Zukoski, who encountered scale effects at all pipe inclinations up to 75°; scale effects did not even diminish at his maximum pipe diameter D = 0.176 m.

Lubbers was the first to systematically investigate the influence of the gas pocket length on the net air discharge (Lubbers 2007, Lubbers and Clemens 2007). He studied the behavior of co-current air-water flows at different configurations (diameter, inclination, slope length, water and air discharge rates) in a laboratory environment using clean water. Pothof has extended Lubbers' experiments to smaller pipe diameters (0.08 m and 0.15 m) in order to quantify scale effects (Pothof and Clemens 2011). Furthermore, Pothof has acquired experimental data in the 40 m long downward sloping section in the Hoek van Holland (HvH) facility, which will be detailed in section 3. A definition sketch for the gas pocket head loss measurements in co-current air-water flow is shown in Figure 1.

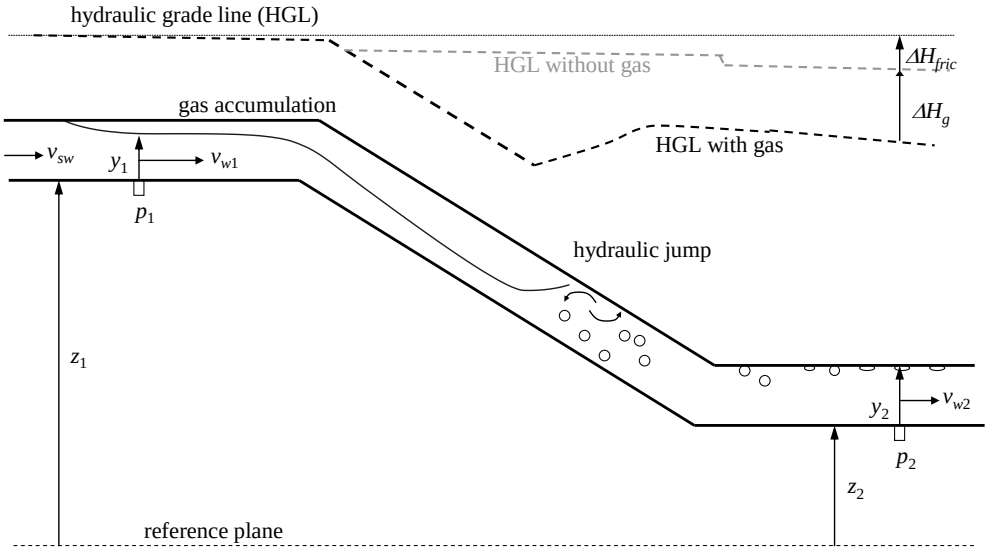

Figure 1: Definition sketch for gas pocket head loss measurements

Pothof has recently developed a numerical model for the total air discharge by flowing water in downward sloping pipes (Pothof and Clemens 2011). This model has been developed and validated against steady state experimental data of co-current flow of air and water. The model will be extended, so that air pocket breakdown experiments can be modeled as well. We will show in this paper that the model is capable of predicting the breakdown rate of a large gas pocket with sufficient accuracy for practical applications. The experimental facility and numerical model are detailed in section 2. Section 3 presents the new breakdown measurements from the large-scale facility at the wastewater treatment plant in Hoek van Holland (HvH). The model performance is discussed in section 4. The conclusions and recommendations are summarized in section 5.

## 2 MATERIALS AND METHODS

### 2.1 Experimental facility for co-current air-water flow measurements

The experimental facility at the wastewater treatment plant in Hoek van Holland (HvH), Netherlands, included an upstream horizontal section with a length diameter ratio $L_{up}/D > 10$ ($D = 192$ mm), a mitre bend into the downward sloping section ($L/D = 209$, $\theta = 10°$), a second mitre bend to a downstream horizontal section, followed by horizontal and rising pipework back to a reservoir with a separation function (Figure 2). This lay-out guarantees that none of the injected air can escape in the upstream direction. The pipe material of the two horizontal sections and the downward sloping reach was transparent PVC.

Figure 2: Overview of HvH facility, shown in upstream direction, with the reservoir in the background ($L$ = 40 m, $\Delta z$ = 7 m, $D$ = 0.192 m)

For the co-current air-water flow measurements, air was injected in the upstream horizontal section. The air mass flow rate was automatically controlled at a pre-set volumetric discharge $Q_g$. The volumetric air discharge was expressed as an air mass flow rate using the water temperature and pressure at the location of the upstream absolute pressure transducer. The upstream absolute pressure $p_1$ was measured in the riser pipe towards the horizontal section. The downstream pressure tapping was located in the downstream horizontal section. This tapping was connected to a second absolute pressure transducer $p_2$. A differential pressure transducer $\Delta p$ was also installed, connected to $p_1$ and the return line.

The water discharge $Q_w$ was measured with an Electro-Magnetic Flow meter (EMF), positioned in the upstream pipe prior to the air injection point. A flow control valve controlled the water discharge to a pre-set value. The air and water discharges were kept constant until the differential pressure reached an equilibrium value; Figure 3 shows a set of equilibrium differential pressures at equilibrium air pocket lengths. At a certain air discharge, the equilibrium differential pressure reduces if the water flow number increases, because the gas pocket length reduces. At large water flow number the gas pocket head loss has become negligible, which is reflected in Figure 3 in datapoints, which coincide with the measured head loss curve without air. Further details of the instrumentation and experiments are found in (Pothof and Clemens 2011).

The actual length of the gas pockets $L_g$ is closely related to the measured gas pocket head loss $\Delta H_g$:

$$\frac{\Delta H_g}{L \sin\theta} \approx \frac{L_g}{L} \text{ or } \quad \Delta H_g \approx L_g \sin\theta \tag{3}$$

where $L$ is the length of the downward sloping section and $\theta$ is the pipe angle. The gas pocket head loss $\Delta H_g$ is determined from the measured differential pressure $\Delta p$ and the differential pressure without air pockets $\Delta p_{fric}$ (i.e. due to friction).

$$\Delta H_g = \left(\Delta p - \Delta p_{fric}\right) \Big/ \rho_w g \tag{4}$$

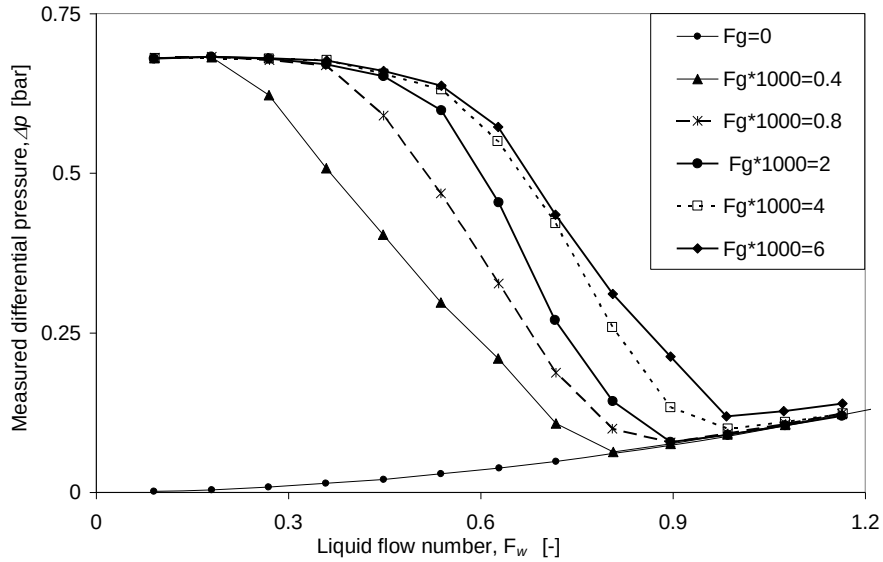


Figure 3: Measured differential pressure in HvH facility in co-current air-water flow

### 2.2 Air discharge model for co-current air-water flow

The air discharge model is based on a new momentum balance on a stationary elongated air pocket in a downwardly inclined pipe (Pothof and Clemens 2010). Pothof and Clemens (2011) have quantified the influence of pipe diameter, length of downward sloping reach, surface tension and viscosity, but the model presented in this paper is a simplified version, valid for air-water flow in long downward sloping reaches ($L > 200D$) and in pipes of sufficient diameter ($D > 0.19$ m). The momentum balance results in a flow number criterion $\mathsf{F}(\theta)$.

$$\mathsf{F}^2(\theta) = \frac{v_{sw}^2}{gD} = \frac{\sin\theta}{\lambda}\frac{D_h}{D}\left(\frac{A_n}{A_D}\right)^2 + \frac{A_D}{A_b}\frac{\cos\theta}{2\pi}\left[\frac{2}{3}\sqrt{\frac{2y_n}{R}-\left(\frac{y_n}{R}\right)^2}\left(\frac{y_n}{R}-3\right)\left(\frac{y_n}{R}-\frac{1}{2}\right)+\arcsin\left(1-\frac{y_n}{R}\right)+\frac{\pi}{2}\right] \tag{5}$$

where $\theta$, $\lambda$, $D_h$, $y_n$ and $R$ are pipe angle, friction factor, hydraulic diameter of the water film, the water film thickness at normal depth and the pipe radius. Furthermore, $A_D$ is the pipe cross sectional area, $A_n$ the wet area at normal depth and $A_b$ the maximum bubble area. The bubble area is maximum when the water phase is flowing at normal depth. Hence

$$A_n + A_b = A_D \tag{6}$$

If the water flow number is just sufficient to prevent any air accumulation in the downward sloping reach, the air flow number $\mathsf{F}_g$ increases exponentially in proportion to the water flow number, following equation (7). This water flow number is referred to as the clearing flow number $\mathsf{F}_c$.

$$\mathsf{F}_g = 1.87\cdot 10^{-7}\exp\left\{9\mathsf{F}_c/\mathsf{F}(\theta)\right\} \tag{7}$$

Equation (7) is valid for air-water flows in pipes with D > 0.19 m. If air accumulates in the downward sloping reach, the influence of the gas pocket head loss follows a cumulative beta distribution function.

$$\mathsf{F}_g = 1.87 \cdot 10^{-7} \exp\left\{9\mathsf{F}_w \Big/ \left(B^{-1}(1-R,\alpha,\beta)\mathsf{F}(\theta)\right)\right\} \tag{8}$$

where

$$1-R = B(x,\alpha,\beta) = \frac{\int_0^x t^{\alpha-1}(1-t)^{\beta-1}\,dt}{\int_0^1 t^{\alpha-1}(1-t)^{\beta-1}\,dt} \tag{9}$$

with

$$\begin{aligned} R &= \Delta H_{gas} \Big/ (L \sin\theta) \\ x &= \mathsf{F}_w / \mathsf{F}_c \\ \alpha &= 6.08 \\ \beta &= 2.39 \end{aligned} \tag{10}$$

The air transport model has been validated with the stationary measurements from the HvH facility and the shorter lab facilities. Figure 4 confirms the reasonable agreement between the numerical model (colored lines) and the HvH data (colored markers) over a wide range of water flow numbers and gas pocket head losses.

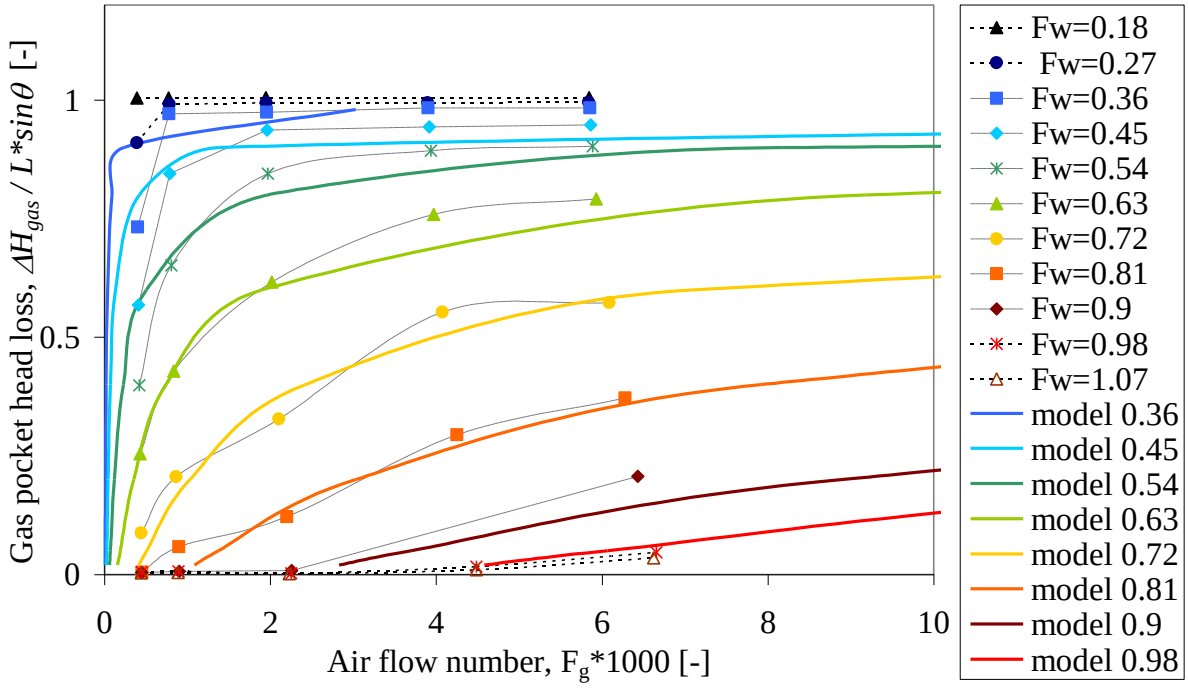


Figure 4: Experimental data-points and numerical results of the gas pocket head loss as a function of the air flow number. Markers show the experimental data from the HvH facility on co-current air-water flow.

Lines show the numerical model performance on the relation between gas pocket head loss and air flow number.

### 2.3 Air pocket breakdown model

The air discharge model, summarized in section 2.2, is a steady state model for the co-current flow of air and water. This model requires an extension for the gas pocket evolution in time in order to use it for air pocket breakdown measurements. The gas pocket length $L_g$ reduces from the tail of the gas pocket, where the water depth is approximately equal to the normal depth. Therefore, equation (11) models the gas pocket length evolution in time, if the absolute pressure would remain constant.

$$A_b \frac{dL_g}{dt} = -\mathsf{F}_g A_D \sqrt{gD} \tag{11}$$

where $A_b$ is the maximum bubble area. According to equations (3) and (4), the gas pocket length and volume are directly related to the gas pocket pressure drop, $\Delta p_g$. Substitution in equation (11) yields an expression for the rate at which the gas pocket pressure difference drops in time.

$$\frac{A_b}{\rho_w g \sin\theta} \frac{d\Delta p_g}{dt} = -\mathsf{F}_g A_D \sqrt{gD} \tag{12}$$

During a break-down experiment, the absolute pressure drops and the air pocket expands, retarding the reduction of the gas pocket head loss. The air transport does not affect the downstream pressure (Figure 5). Therefore, the reduction of the gas pocket head loss is completely reflected in the reduction of the upstream absolute pressure. Hence, the absolute pressure in the top of the downward sloping pipe, denoted by $p_{top}$, follows the same evolution in time as the gas pocket pressure drop.

$$\frac{A_b}{\rho_w g \sin\theta} \frac{dp_{top}}{dt} = -\mathsf{F}_g A_D \sqrt{gD} \tag{13}$$

In the numerical model with time step *dt*, the new gas pocket pressure drop and absolute top pressure are predicted from equations (12) and (13); these predictions are indicated with subscript *pred*. The air expansion is calculated in a second step from the isothermal gas law (p·V=C), using the observation from equation (3) that the air volume is linearly related to the gas pocket pressure drop.

$$\begin{aligned} & p_{top,pred} \cdot \Delta p_{g,new} = p_{top} \cdot \Delta p_{g,pred} \\ & \Leftrightarrow \\ & \left( p_{top} - \frac{\mathsf{F}_g A_D \sqrt{gD} \rho_w g \sin\theta}{A_b} dt \right) \cdot \Delta p_{g,new} = p_{top} \cdot \left( \Delta p_g - \frac{\mathsf{F}_g A_D \sqrt{gD} \rho_w g \sin\theta}{A_b} dt \right) \end{aligned} \tag{14}$$

It is noted that this model neglects the expansion of air in the upstream horizontal section, but the air volume in this section is small compared to the air volume in the downward sloping reach, especially if $\mathsf{F}_w > 0.582$ when the air bubble shape resembles a free outflow from a horizontal pipe (Hager 1999).

The air pocket breakdown measurements in the HvH facility were carried out in accordance with the following procedure:

1. The water discharge was set to a low discharge of approximately 10 l/s.
2. The air discharge was set to its maximum value (appr. 0.9 nl/s) in order to render a rapid accumulation of the air pocket.
3. When the air pocket reached the bottom of the inclined section, the water discharge was set to its desired value, at which the breakdown measurement would be carried out.
4. Then the air discharge was stopped. The following water flow numbers were evaluated: $\mathsf{F}_w$ = (0.39; 0.63; 0.75 and 0.94)

## 3 RESULTS

The breakdown data (25 s average values) at a water flow number $F_w$ = 0.63 or discharge $Q_w$ = 25 l/s are shown in Figure 5. The water discharge is kept constant by the flow control valve. The exponential decay in the differential pressure and in the pressure at the top of the downward sloping section confirm the decaying trend in the air discharge. The air discharge is not large enough to have any effect on the downstream pressure, which remains constant during the entire experiment.

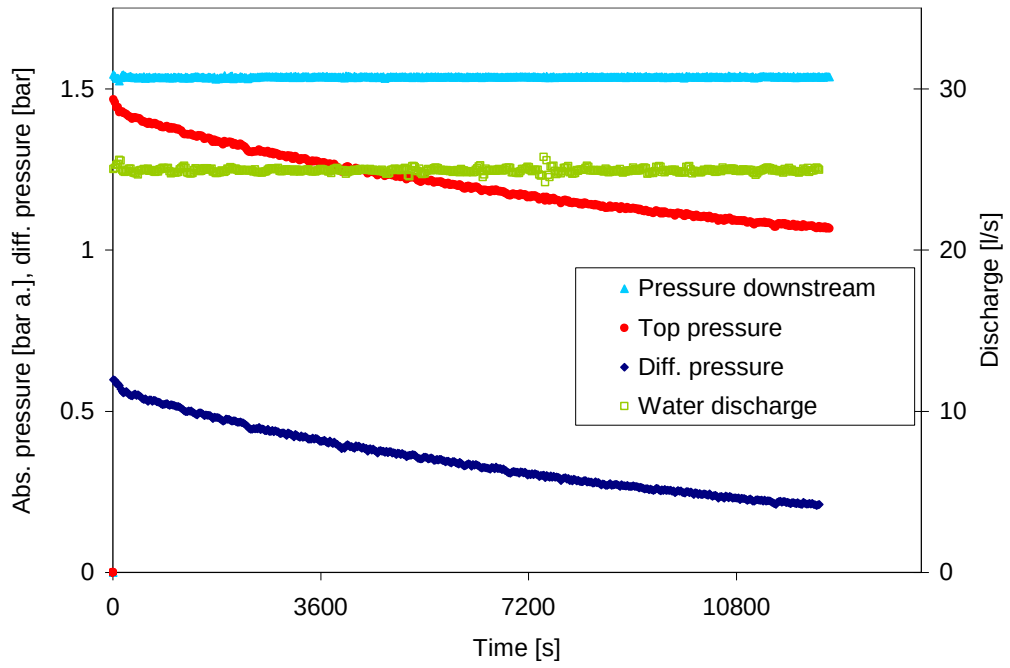


Figure 5: Breakdown experiment at $F_w$ = 0.63

Figure 6 shows a comparison of the breakdown experiments and the air pocket breakdown model. At relatively large air pocket volumes, the air discharge model overpredicts the actual breakdown rate. At smaller gas pocket volumes, within the validated range of the stationary co-current air-water flow measurements ($F_g$ < 0.01), the breakdown model predicts the measured breakdown rate reasonably well. The observed differences are discussed in detail in section 4.

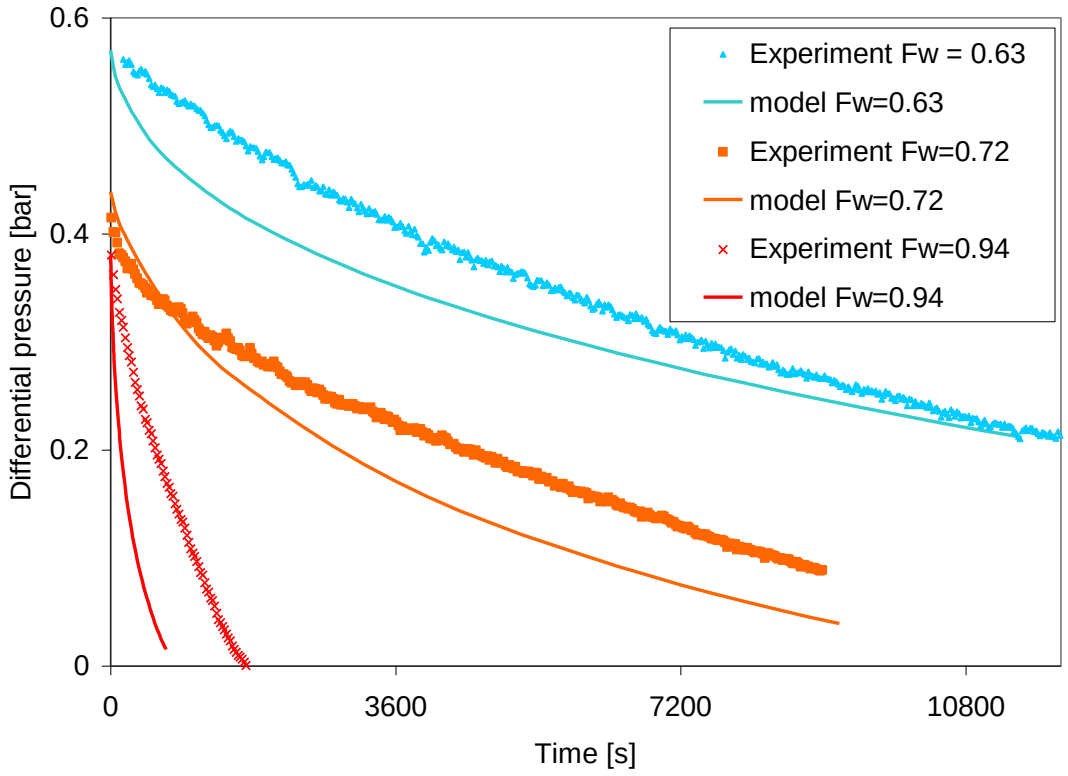


Figure 6: Gas pocket pressure drop evolution during air pocket breakdown experiments at $F_w = 0.63$, $F_w = 0.72$ and $F_w = 0.94$. The symbols denote the measurements, the lines denote the model results.

## 4 DISCUSSION

The model simulations yield a reasonable prediction of the air pocket breakdown and removal process. A number of phenomena explain the observed differences between the measured and computed gas pocket pressure loss:

1. The validated range of the air transport model
2. The approximate relation between air pocket length and air pocket head loss
3. The computed normal depth

Each of these items will be addressed in the following paragraphs.

The validated range of the air transport model is limited to air flow numbers $F_g < 0.01$ as illustrated in Figure 4. The computed air flow numbers during the initial stage of the breakdown experiments are an order of magnitude larger, especially at the largest water flow number $F_w = 0.94$. Over the investigated range of air discharges, the air discharge increases exponentially in the water discharge at a given gas pocket head loss (eq. (7)). Apparently, the exponential increase cannot be extrapolated to air discharges that are one order of magnitude larger than evaluated. Furthermore, Figure 6 shows that the model overpredicts the actual air discharge at a water flow number $F_w = 0.94$.

The air pocket volume is subdivided in multiple air pockets with air-entraining hydraulic jumps, if the water flow number $F_w > 0.58\cos\theta$, following (Pothof and Clemens 2010). Some pressure recovery

occurs in these hydraulic jumps. This effect implies that the actual gas pocket volume is larger than estimated from equation (3). The real breakdown rate will therefore be smaller than the computed breakdown rate, if this effect is not accounted for.

Finally, the computed normal depth may differ from the actual water depth underneath the air pockets. If one of the air bubbles in the downward sloping reach is smaller than 9D, normal depth is not reached at the tail of this air bubble. Therefore, the actual air pocket break down rate will be greater than predicted. This argument is believed to be of minor importance for a couple of reasons: first, it contradicts the generally observed trend that the predicted air pocket breakdown rate exceeds the measured breakdown rate and, secondly, the air pockets in the breakdown measurements at $F_w = 0.63$ and $F_w = 0.72$ are much longer than 9D during the experiments. This argument may play a minor role at the largest water flow number.

## 5 CONCLUSIONS

The recently developed stationary numerical model for the total air discharge by flowing water in downward sloping pipes has been summarized and compared with available experimental data. The model has been extended, so that the dynamic evolution of the air pocket breakdown process can be simulated. New experimental data on the breakdown of large gas pockets have been presented. The experimental results have been compared with the numerical model. The main conclusion is that the numerical model predicts the gas pocket breakdown rate with reasonable accuracy for practical applications, especially when the predicted air discharge is within the validated range; i.e. $F_g < 0.01$. The numerical model is a useful tool to assess how long it may take to breakdown an accumulation of air in a downward sloping pipe. The model may be applied in wastewater engineering (downward sloping pipes), bottom outlets or stormwater storage tunnels (during priming events).

## 6 ACKNOWLEDGMENTS

This work was part of the joint industry project CAPWAT on capacity reduction in pressurised wastewater mains. The CAPWAT project was funded by Deltares, Delft University of Technology, water boards Delfland, Hollands Noorderkwartier, Brabantse Delta, Reest en Wieden, Rivierenland, Zuiderzeeland, Fryslân and Hollandse Delta, water companies Aquafin and Waternet, consultants Royal Haskoning, Grontmij Engineering Consultancy, Gemeentewerken Rotterdam, pump manufacturer ITT Water & Wastewater, R&D foundations STOWA and RIONED and the Dutch Ministry of Economic Affairs. More information is available on-line at http://capwat.deltares.nl and http://www.youtube.com/capwat.

## 7 REFERENCES

Bendiksen, K. H. (1984). Experimental investigation of the motion of long bubbles in inclined tubes. *International Journal of Multiphase Flow 10*(4), 467-483.

Capart, H., Sillen, X., Zech, Y. (1997). Numerical and experimental water transients in sewer pipes. *J. Hydr. Res. 35*(5), 659-672.

Escarameia, M. (2007). Investigating hydraulic removal of air from water pipelines. *Proceedings of the Institution of Civil engineers: Water Management 160*(1), 25-34.

Gandenberger, W. (1957). *Über die wirtschaftliche und betriebssichere Gestaltung von Fernwasserleitungen*. München: R. Oldenbourg Verlag.

Hager, W. H. (1999). Cavity outflow from a nearly horizontal pipe. *International Journal of Multiphase Flow 25*(2), 349-364.

Kalinske, A. A., Bliss, P. H. (1943). Removal of air from pipe lines by flowing water. *Proceedings of the American Society of Civil Engineers (ASCE) 13*(10), 3.

Kent, J. C. (1952). *The entrainment of air by water flowing in circular conduits with downgrade slope*. University of Berkeley, Berkeley, California.

Lubbers, C. L. (2007). *On gas pockets in wastewater pressure mains and their effect on hydraulic performance.* Delft University of Technology, Delft.

Lubbers, C. L., Clemens, F. H. L. R. (2007). Scale effects on gas transport by hydraulic jumps in inclined pipes; comparison based on head loss and breakdown rate, *6th Int. Conference on Multiphase Flow (ICMF)*. Leipzig.

Pothof, I. W. M., Clemens, F. H. L. R. (2010). On elongated air pockets in downward sloping pipes. *Journal of Hydraulic Research 48*(4), 499 - 503.

Pothof, I. W. M., Clemens, F. H. L. R. (2011). Experimental study of air-water flow in downward sloping pipes. *Int. J. of Multiphase Flow 37*, 278 - 292.

Vasconcelos, J. G., Wright, S. J. (2009). Investigation of rapid filling of poorly ventilated stormwater storage tunnels. *Journal of Hydraulic Research 47*(5), 547 - 558.

Wickenhäuser, M., Kriewitz, C. R. (2009). Air-Water Flow in Downward Inclined Large Pipes, *33rd IAHR Congress: Water Engineering for a Sustainable Environment*. Vancouver: IAHR.

Zukoski, E. E. (1966). Influence of viscosity, surface tension, and inclination angle on motion of long bubbles. *Journal of Fluid Mechanics 25*(4), 821-837.